Magnetic fluctuations in $Eu_2BaZn_xNi_{1-x}O_5$ Haldane systems

J. van Lierop,[1] C. J. Voyer,[2] T. N. Shendruk,[1] D. H. Ryan,[2] J. M. Cadogan,[3] and L. Cranswick[4]
[1]*Department of Physics and Astronomy, University of Manitoba, Winnipeg, Manitoba, Canada R3T 2N2*
[2]*Centre for the Physics of Materials and Physics Department, McGill University, Montréal, Quebec, Canada H3A 2T8*
[3]*School of Physics, The University of New South Wales, Sydney, NSW, Australia*
[4]*Canadian Neutron Beam Centre, Chalk River Laboratories, Chalk River, Ontario, Canada K0J 1J0*
(Received 20 December 2005; published 5 May 2006)

The Ni^{2+} ions in Eu_2BaNiO_5 form antiferromagnetic Heisenberg $S=1$ chains with a Haldane gap. Replacing Ni^{2+} with Zn^{2+} decreases the average Ni^{2+} chain length. ^{151}Eu and ^{153}Eu Mössbauer spectroscopy have been used to study the chain length dependence of the magnetism in $Eu_2BaZn_xNi_{1-x}O_5$ with $x=0, 0.05$, and 0.1. Using exchange-induced Eu^{3+} moments these independent and complementary local probes of the magnetism reveal that the chain moments undergo temperature dependent fluctuations where shorter chain lengths exhibit faster fluctuations at any given temperature. The Eu^{3+} antiferromagnetic order is established at $T_N \sim 5$ K, independent of the Ni^{2+} chain length. Thermally activated moment fluctuations are observed above T_N. Chain cutting increases the molecular exchange field of the Ni^{2+} on the Eu^{3+} and indicates a polarization of Ni^{2+} interdimer coupling in the quantum spin chains.

DOI: 10.1103/PhysRevB.73.174407 PACS number(s): 76.75.+i, 75.50.Lk, 75.50.Tt

I. INTRODUCTION

Mixed spin quantum systems provide a fascinating look into the coexistence of different types of magnetic ordering with excitations that lead to interesting competing effects. The family of mixed spin quantum systems based on R_2BaNiO_5 (where R is a magnetic rare earth ion) are of particular interest as three dimensional long range magnetic ordering coexists with one-dimensional Haldane quantum spin gap excitations.[1] These linear chain rare earth nickelates have an $S=1$ Haldane subsystem composed of Ni^{2+} ions that undergo a strong and essentially isotropic nearest-neighbor antiferromagnetic exchange interaction. In a perfect Haldane configuration, the isolated $S=1$ spin chains have a gap in the magnetic excitation spectrum, but do not exhibit any long range order, even at $T=0$ K, as quantum fluctuations dominate the behavior. However, three-dimensional (antiferromagnetic) long range ordering occurs in the R_2BaNiO_5 system through exchange coupling of magnetic R^{3+} ions by way of the dynamical polarization of the Ni^{2+} chains.[2] The coexistence of the three-dimensional magnetic ordering of the R^{3+} sublattice with the one-dimensional antiferromagnetically coupled Ni^{2+} quantum spin chains provides a staggered field on the Ni^{2+} chains. The magnitude of this staggered field can be tuned using either R^{3+} moment size (p) or temperature, and the ordering temperature of the $R^{3+}(T_N)$ should track with the estimated spin component (ignoring crystal field effects)[3] as the R^{3+}-R^{3+} interactions are much weaker than the R^{3+}-Ni^{2+} interactions. Some insight into the interactions that dominate the R^{3+} ordering process can be obtained by examining the ordering temperature (T_N) dependence on p^2 (inset to Fig. 1). A linear trend of T_N with p^2 suggests that R^{3+}-R^{3+} coupling is responsible for ordering, which is observed for the R_2BaNiO_5 where the rare-earth has a low f-electron occupancy (i.e., R=Sm, Nd, Gd, Tb, and Dy in order of increasing p) exhibited by the systems with high T_N (inset to Fig. 1). While this trend could indicate that the R^{3+}-Ni^{2+} interactions are isotropic, for the R^{3+} with further increasing f-electron shell occupancy, the magnetic ordering is clearly more complex. An exponential increase of T_N with p^2 (inset to Fig. 1) distinguishes a different interaction between the R^{3+}-R^{3+} as well as the R^{3+}-Ni^{2+} in the systems with R=Ho, Er, Tm, and Yb in order of decreasing p.

Of all rare earth ions examined in these nickelate systems, studies with R=Eu have presented some of the most intriguing magnetism. Eu^{3+} is a $J=0$ ion and should, therefore, have zero effective magnetic moment. Nonetheless, optical spectroscopy studies suggested a magnetic ordering around 20 K,[5] and recent ^{151}Eu Mössbauer measurements[6] have been interpreted to yield $T_N=30$ K. Both of these T_N values lie essentially halfway from either T_N versus p^2 trends de-

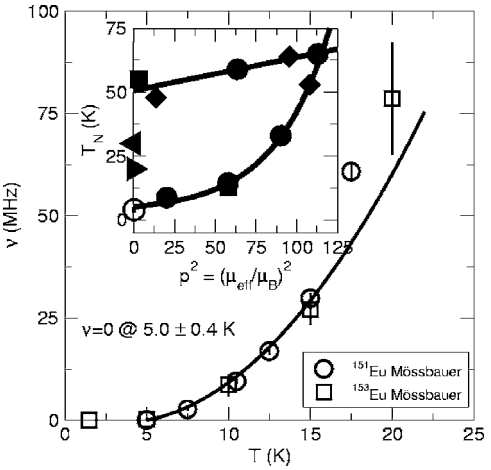

FIG. 1. Eu^{3+} moment fluctuation rate as a function of temperature in Eu_2BaNiO_5 determined from the fitted ^{151}Eu and ^{153}Eu Mössbauer spectra (Ref. 4). Solid line is a fit as described in the text. Inset: Ordering temperature, T_N, as a function of the square of the rare earth moment size, $p^2=g_J[J(J+1)]=(\mu_{eff}/\mu_B)$ (Ref. 2) in R_2BaNiO_5. ● Mössbauer spectroscopy, ■ optical spectroscopy, ◆ neutron diffraction (see Ref. 3 and references therein). Eu_2BaNiO_5 results: ○ this work, ▶ optical measurements (Ref. 5), ◀ ^{151}Eu Mössbauer analysis (Ref. 6). Solid lines are a guide to the eye.

scribed above and are significantly above anything expected from the R^{3+}-Ni^{2+} interaction dependence of T_N with the rare earth exchange energy.[6]

Together with the problem of assigning T_N for Eu_2BaNiO_5 is the issue of determining the R moment size for Eu^{3+}. Knowledge of the moment size is required to determine correctly the effects of the staggered field on the three-dimensional antiferromagnetic ordering in the presence of the Haldane system. A smaller than usual interval between the ground ($J=0$) and the first excited state occurs for Eu^{3+}, leading to a significant population of Zeeman states that creates a none zero $p=\mu_{eff}/\mu_B$. Hund's rule for the $J=0$ Eu^{3+} ion yields $p=0$, while thermal population of the Zemann states results $p=3.34$, the typical experimental value.[7] There is a strong temperature dependence to the value of p in the Eu-based oxides (consistent with a thermally driven mixture of states), so neutron diffraction has been used to set an upper bound for p in our Eu_2BaNiO_5 sample.

Since optical measurements of T_N in Eu_2BaNiO_5 (Ref. 5) involve dipole transitions that occur on a timescale of $10^{-7}-10^{-9}$ s, it is possible that the apparent $T_N=20$ K may only be an effective *dynamical* freezing temperature of the moment fluctuations on a nanosecond time scale, and that the true, static transition occurs at a significantly lower temperature. ^{151}Eu Mössbauer measurements[6] were also interpreted in terms of a temperature dependent *static* distribution of Eu^{3+} hyperfine fields induced by ordered Ni^{2+} chain moments and this analysis led to $T_N=30$ K. However, static disorder and dynamic effects can yield very similar Mössbauer spectral patterns[8] and a unique separation of static and dynamic magnetism is often problematic. Indeed, the very large difference between the two T_N derived from methods with quite different natural timescales, itself suggests that dynamic effects are playing a significant role. Finally, inelastic neutron scattering experiments on R_2BaNiO_5[1,9] have shown that there are substantial dynamic magnetic interactions between the Ni^{2+} quantum spin chains and the R^{3+} subsystem in addition to the expected static magnetic interactions. Recent quantum Monte Carlo studies also point to the importance of fluctuations.[2]

It is clear that static and dynamic views of the magnetism in Eu_2BaNiO_5 imply conceptually different underlying behavior. To properly resolve the contradictions surrounding these diametrically opposed interpretations, we have employed basic magnetic characterization in concert with both ^{151}Eu and ^{153}Eu Mössbauer spectroscopy. The two europium isotopes probe exactly the same exchange-induced Eu^{3+} moments in an independent and complementary manner and must, therefore, reflect the same distribution of static hyperfine fields or the same time-dependent magnetism in Eu_2BaNiO_5. Moreover, the Mössbauer measurements provide a measure of the Ni^{2+} moments in the quantum spin chains by way of the exchange-induced Eu^{3+} moments. Finally, an open question in R_2BaNiO_5 systems is how the Ni^{2+} quantum spin chain length affects the static and time-dependent magnetism. We address this issue by decreasing the average Ni^{2+} chain length by doping the Eu-nickelate system with nonmagnetic Zn^{2+} ions (on-site chain substitution), and have examined the static and dynamic magnetism in $Eu_2BaZn_xNi_{1-x}O_5$ with $x=0.05$ and 0.1.

We find that the broad hyperfine field distribution apparent in earlier work[6] is entirely due to the dynamic effects of moment fluctuations with a temperature dependence that is consistent with a thermally activated process. Both ^{151}Eu and ^{153}Eu Mössbauer measurements yield the same Ni^{2+} moment size. Furthermore, the Eu moments become static and ordered below $T_N\sim 5$ K for all x in $Eu_2BaZn_xNi_{1-x}O_5$. This behavior is in agreement with the rare-earth exchange energy,[6] and provides strong evidence that the R^{3+}-Ni^{2+} interaction governs the rare-earth exchange energy in this system. Moreover, Zn^{2+} doping leads to increases in both the proportion of paramagnetic Ni^{2+} ions (shorter Ni^{2+} chains) and the magnetic fluctuation rate above T_N. Finally, Zn^{2+} substitution seems to increase the molecular exchange field of the Ni^{2+} on the Eu^{3+}, with a concomitant $\sim$25% increase in the average Ni^{2+} moment size.

II. EXPERIMENTAL METHODS

$Eu_2BaZn_xNi_{1-x}O_5$ was prepared by mixing stoichiometric amounts of Eu_2O_3 (REacton, 99.9% pure), $BaCO_3$ (Aldrich, 99.999% pure), Zn (Johnson Matthey, 99.999% pure), and NiO (Aldrich, 99.99% pure), heating in air to 1170 K for 24 h. The powder was then pressed into a pellet and fired in air at 1270 K for 24 h. The pellet was then repeatedly ground, pressed, and fired at 1370 K until all x-ray visible impurities disappeared. Cu $K\alpha$ x-ray diffraction was used to determine the structure of the compounds. Basic magnetic characterization was carried out on a commercial susceptometer/magnetometer. ^{151}Eu transmission Mössbauer spectra were collected on a constant acceleration spectrometer using a 4 GBq $^{151}SmF_3$ source. The spectrometer was calibrated using ^{57}Co and α-Fe. ^{153}Eu transmission Mössbauer spectra were collected on a laser-calibrated spectrometer operated in sine-mode using a 1 GBq $^{153}Sm_2O_3$ source that was obtained by neutron irradiating $^{152}Sm_2O_3$ (98%+ pure isotope). All spectra were collected in a helium flow cryostat. Linewidths (HWHM) for the ^{151}Eu ($\Gamma_{nat}=1.337\pm0.006$ mm/s) and ^{153}Eu ($\Gamma_{nat}=0.627\pm0.002$ mm/s) Mössbauer sources were determined using a $Eu_3Fe_5O_{15}$ standard.

The extremely high thermal neutron absorption cross section of europium ($\sigma_{abs}=4350$ b) makes diffraction measurements with conventional cylindrical sample geometries impractical. We, therefore, built a large-area flat-plate mount using two 1 mm thick single crystal Si wafers separated by a 75 μm vanadium gasket.[10] The holder was loaded with $\sim$1 g of powdered sample spread over a 2 cm$\times$8 cm area, for a calculated transmission of $\sim$40% at normal incidence. Neutron powder diffraction experiments were carried out on the 800-wire C2 high-resolution powder diffractometer located at the NRU reactor, Chalk River, and operated by the Canadian Neutron Beam Centre. Temperatures down to 3.6 K were obtained using a closed-cycle refrigerator. The neutron wavelength used was 2.3719 Å and the sample plane was oriented perpendicular to the beam in order to optimize transmission for the expected low-angle magnetic peaks.

III. RESULTS AND DISCUSSION

A. Basic magnetic characterization and the Eu^{3+} moment

X-ray diffraction structural characterization of Eu_2BaNiO_5 is shown in Fig. 2. Similar results were obtained

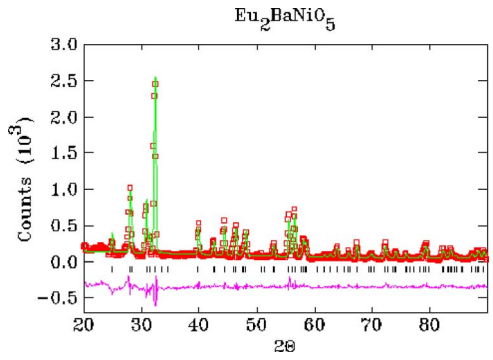

FIG. 2. (Color online) X-ray diffraction data and fit results with residuals (bottom) for the Eu_2NiBaO_5 sample.

on the $Eu_2BaZn_xNi_{1-x}O_5$ with $x=0.05$ and 0.1. Diffraction patterns were fitted using the GSAS[11]/EXPGUI[12] package where an orthorhombic crystal structure with space group *Immm* and cell constants $a=3.7992(6)$ Å, $b=5.8488(9)$ Å, and $c=11.4961(19)$ Å resulted in the best fit to the data. These values are consistent with those obtained from the other R_2BaNiO_5 systems.[1]

The temperature dependence of the dc susceptibility, $\chi(T)$, in a field of 0.01 T for the $Eu_2BaZn_xNi_{1-x}O_5$ samples is shown in Fig. 3. The experimental data have been corrected by taking into account a paramagnetic, Curie-law contribution that is typical of powder R_2BaNiO_5 samples.[13,14] The impact of the Haldane gap on $\chi(T)$ is clearly seen by way of the marked minimum around 25 K. The Curie-Weiss behavior of $\chi(T)$ apparent below 20 K has been observed in other R_2BaNiO_5 systems[1,13,14] and indicates that low lying excited states of the Eu^{3+} ions with nonzero J are interacting with the Ni^{2+} quantum spin chains, resulting in an effective Eu moment.

Theory of Haldane gap antiferromagnets in an applied field has indicated that the low temperature exponential susceptibility is due to symmetry breaking of the single particle states that results in the splitting of the Haldane gap, with a $\chi(T) \propto \sqrt{T\Delta}\exp(-\Delta/T)$[15,16] from which follows the phenomenological description of $\chi(T)$ in R_2BaNiO_5 (Ref. 14)

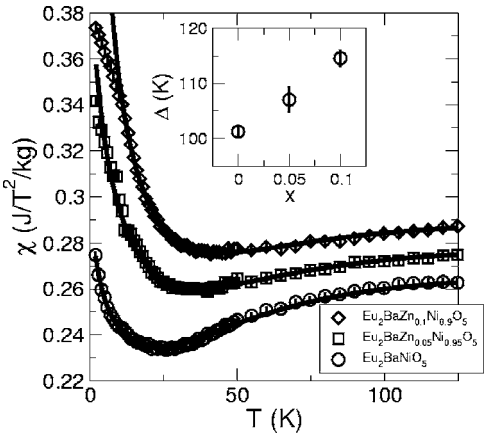

FIG. 3. DC susceptibility (χ) of the $Eu_2BaZn_xNi_{1-x}O_5$ with $x=0$ (○), 0.05 (□), and 0.1 (◇) as a function of temperature, T. Solid lines are fits described in the text. Inset: Results of data fitted using Eq. (1).

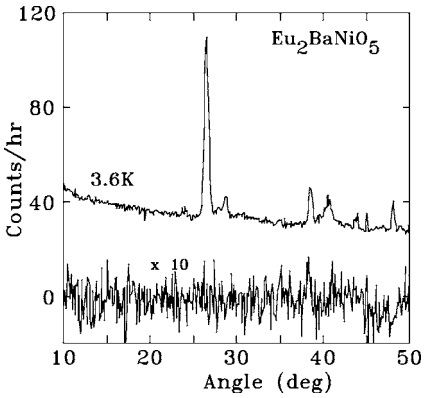

FIG. 4. Neutron diffraction data for Eu_2BaNiO_5 at 3.6 K at a wavelength of 2.37 Å. The lower curve shows the difference between the pattern at 50 and 3.6 K scaled up by a factor of ten to emphasize the absence of intensity changes that could be attributed to magnetic ordering.

$$\chi(T) = \chi_0 + \frac{C}{T+\Theta_W} + a\sqrt{T\Delta}\exp(-\Delta/T), \qquad (1)$$

where χ_0 is a constant part of the susceptibility, C is a Curie-Weiss term with Θ_W the Weiss temperature, a a fitting constant, Δ the energy gap of the one-dimensional quantum spin chain, and T the temperature.

The pure Eu_2BaNiO_5 (○ in Fig. 3) is well represented by a nonlinear least squares fit with Eq. (1) (solid line in Fig. 3) over the appropriate temperature range up to $T\sim\Delta$,[16] and indicates $\Theta_W=4\pm1$ K which is in good agreement with similar Haldane systems.[14] Furthermore, Δ (inset in Fig. 3 for $x=0$) is in excellent agreement with inelastic neutron scattering measurements of the Haldane gap energy in other R_2BaNiO_5 systems.[1]

The dc susceptibility results establish that we have a Haldane system with an identification of Δ and Θ_W that is compatible with other R_2BaNiO_5. It is now necessary to ascertain the R moment size to establish the effect of the staggered field on the quantum spin chains and the scaling of T_N versus p^2 for Eu_2BaNiO_5. We turn to neutron diffraction results obtained at 3.6 and 50 K. Comparison of these neutron diffraction data at these two temperatures shows no additional scattering on cooling (Fig. 4) that could be attributed to magnetic ordering. The weak overall scattering and rather high absorption of europium coupled with the relatively small atomic moments likely placed the signal at the limit of our sensitivity, even after ten days of data collection. Magnetic scattering patterns were calculated using FULLPROF[17] in order to determine upper limits for the Ni^{2+} and Eu^{3+} moments. The $\langle j_0\rangle$ magnetic form factor coefficients for Eu^{3+} were taken from Table 3 of Brown's article[18] as they are not built in to FULLPROF. We assumed a propagation vector of $[\frac{1}{2}\ 0\ \frac{1}{2}]$, typical of R_2BaNiO_5 compounds,[19] with Eu and Ni moments ordered parallel to either the a-axis or the c-axis. The calculated intensities were normalized to the strong nuclear peak at $2\theta\sim26.5°$ and then compared with the uncertainties in possible magnetic peaks at $2\theta=19.0°$, 30.3°,

and 34.9° in order to put limits on possible Eu^{3+} and Ni^{2+} moments. Independent of the assumed ordering direction we obtain upper limits of: $\mu_{Eu^{3+}} < 0.4\ \mu_B$ and $\mu_{Ni^{2+}} < 0.7\ \mu_B$ at 3.6 K. As the Mössbauer data imply a Eu^{3+} moment of about 0.18 μ_B[6,20] (see below) it is well below our detection limit, however, typical Ni^{2+} are of order 1 μ_B so we might have expected to see some magnetic scattering from the nickel chains. It is clear that a substantially greater integrated intensity and probably lower temperatures would be needed to observe either Ni^{2+} or Eu^{3+} moments in this material. Finally, these neutron diffraction results show that the T_N for Eu_2BaNiO_5 (○ in Fig. 1 inset) is consistent with the scaling of T_N versus p for the other R_2BaNiO_5 (solid line in Fig. 1 inset).

Replacing the Ni^{2+} with nonmagnetic Zn^{2+} has a significant effect on $\chi(T)$. For $Eu_2BaZn_xNi_{1-x}O_5$, the magnitude of the Curie-Weiss moment increases with x as does the contribution from the low temperature paramagnetic component. Furthermore, there is a suppression of the effect of the Haldane gap on $\chi(T)$, with the minimum in $\chi(T)$ becoming less pronounced with increasing x. Zero field-cooled and field-cooled temperature scans for all x showed no history dependent susceptibility, consistent with on-chain site substitution[21] and a strong indication that the broken Ni^{2+} chains are isolated from each other with no chance of magnetic ordering from superexchange interactions between chain ends.

Fitting $\chi(T)$ for the doped samples using Eq. (1) shows a steady increase in Δ with x (Fig. 3 inset). Nonmagnetic impurities produce quantum spin chain segments of finite lengths, and numerical studies of $S=1$ Heisenberg chains have shown that decreasing the chain length leads to an increase in the Haldane gap energy[22] due to an effective renormalization of the gap energy. Indeed, the effects of substitutional chain breaking are exhibited by the measured increase in Δ, as the nonmagnetic impurities decrease the average $S=1$ quantum spin chain length.

The first indications that the magnetism in $Eu_2BaZn_xNi_{1-x}O_5$ may be time dependent come from the frequency dependence of $\chi_{ac}(T)$ shown in Fig. 5. Temperatures in the 100–200 K regime (above the gap energy, Δ) exhibit the strongest frequency dependence. At temperatures below Δ, a smaller frequency variation is observed. For temperatures that are larger than that set by the Haldane gap energy, a large fraction of the measured moment fluctuations are rapid with a relatively small fraction of moment fluctuations occurring at slower rates (hence the larger 10 kHz χ_{ac} than 100 Hz χ_{ac} shown in Fig. 5). With cooling to temperatures at and below the same scale as the Haldane gap energy, the average moment fluctuation in the material slows such that there is less difference between different measuring times. This frequency dependence of χ_{AC} suggests dynamical freezing is happening in these materials and that an explicit time-dependence should be incorporated into our description of the physics of the magnetism in $Eu_2BaZn_xNi_{1-x}O_5$.

However, it is the ^{151}Eu and ^{153}Eu Mössbauer data that provide the clearest evidence of time dependent moment fluctuations on the Ni^{2+} ions in the quantum spin chains. While the two isotopes provide independent information on

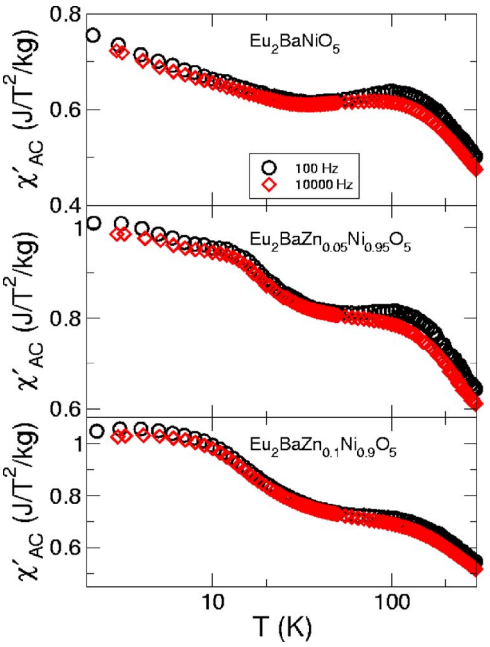

FIG. 5. (Color online) AC susceptibility (χ'_{ac}) of the $Eu_2BaZn_xNi_{1-x}O_5$ with $x=0$ (top), 0.05 (middle), and 0.1 (bottom) as a function of temperature, T. A 10 mT drive field was used during the 100 Hz (○) and 10 kHz (◇) measurements. The paramagnetic contribution to the susceptibility has not been subtracted from these data.

precisely the same property, namely the magnetic hyperfine field at the Eu nucleus, they have quite different field sensitivities and natural timescales. As a result, only a consistent treatment of the magnetic behavior in $Eu_2BaZn_xNi_{1-x}O_5$ will provide agreement between data sets from the two isotopes.

B. Eu_2BaNiO_5

Consider the 5 K ^{151}Eu and ^{153}Eu Mössbauer spectra of Eu_2BaNiO_5, shown in Fig. 6. Previous optical[5] and ^{151}Eu Mössbauer[6] work place T_N well above 5 K and we should, therefore, observe the static, ordered state for both spectra. The combination of significantly broadened spectral lines (compared to their natural linewidths) and observed line positions shows clear evidence of a distribution of hyperfine fields at the different Eu nuclei in Eu_2BaNiO_5. This observation is most simply described by a static distribution of hyperfine fields, $P(B_{hf})$, that is combined with the correct hyperfine parameters for ^{151}Eu and ^{153}Eu and line intensities proportional to the appropriate Clebsch-Gordan coefficients.[23] Using Window's method[24] to calculate $P(B_{hf})$, results of fits to the low temperature spectra are shown in Fig. 6 as solid lines in the left panels with the hyperfine field distribution for both isotopes being shown to the right. This static model yields a fair fit to the spectra, but there are clear mis-fits (e.g., the left-most line in the ^{151}Eu pattern at ~−7 mm/s is missed). More importantly, the two derived field distributions *do not match*. Our $P(B_{hf})$ for ^{151}Eu is strikingly similar to that obtained previously,[6] but $P(B_{hf})$ for the ^{153}Eu Mössbauer spectrum is very different. As both Möss-

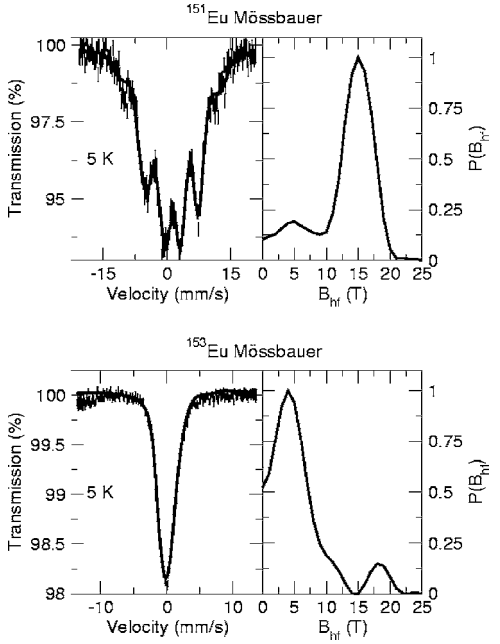

FIG. 6. ^{151}Eu (top) and ^{153}Eu (bottom) Mössbauer spectra of Eu_2BaNiO_5 at base temperature fitted with a distribution of static hyperfine fields $[P(B_{hf})]$ shown at right. Solid lines are static fits described in the text.

bauer isotopes of europium are necessarily exposed to precisely the same magnetic environment, the only way to reconcile the different $P(B_{hf})$ for the two isotopes is to assume that the physical description of the magnetism being used in the static fits is incorrect.

These results demand an alternate physical description of the Eu^{3+} moment temperature evolution (and hence the Ni^{2+} quantum spin chain development). As a static magnetic description is clearly incorrect, dynamic effects must be considered. This move is also consistent with the $\chi_{ac}(T)$ frequency dependence described above.

Instead of using a static hyperfine field $P(B_{hf})$, spectra were fitted with a modified two-level magnetic relaxation Blume and Tjon[4,25] formalism. With the correct hyperfine parameters for ^{151}Eu and ^{153}Eu and line intensities proportional to the appropriate Clebsch-Gordon coefficients,[23] a consistent description of the temperature evolution of the magnetism shown in Fig. 7 was achieved.

Fits using this model are shown as the solid lines in Fig. 7. The lowest temperature spectra were used to determine the linewidth Γ, isomer shift IS, quadrupole splitting QS and magnetic hyperfine field B_{hf}. The temperature evolution of the spectra was then described entirely by changes in the fluctuation rate of the Eu moment, ν. $\Gamma=1.3(3)$ mm/s for the 5 K ^{151}Eu spectrum and $\Gamma=0.63(7)$ mm/s for the 1.5 K ^{153}Eu spectrum, are in excellent agreement with the experimentally determined source linewidths (see above). Two subspectra were required to fit the base-temperature spectra (Fig. 8). ~90% of the spectral area required a combination of quadrupole and magnetic interactions, while the remaining 10% showed only a quadrupole interaction. The 10% nonmagnetic contribution is consistent with the paramagnetic fraction of the sample seen in $\chi(T)$ (○ for $x=0$ in Fig. 3).

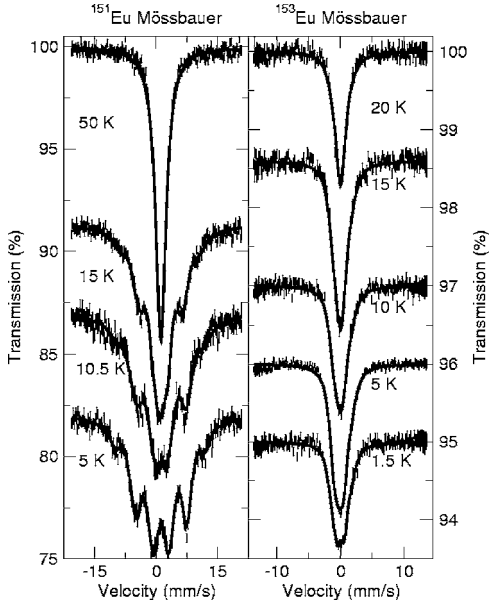

FIG. 7. Typical ^{151}Eu (left panel) and ^{153}Eu (right panel) transmission Mössbauer spectra of Eu_2BaNiO_5. Solid lines are dynamic fits as described in the text.

This paramagnetic component indicates the presence of Ni^{2+} chain defects,[1,6] and is in agreement with our analysis of the $\chi(T)$ data. It is important to note that the fitted IS ~1.2 mm/s is consistent with the nonmagnetic Eu^{3+} $^7F^0$ ground state,[23] which is further evidence that the measured Eu moment arises by way of exchange coupling to the Ni^{2+} ions in the Haldane quantum spin chains and is not due to either Eu^{2+} impurities or valence fluctuations.

B_{hf} for the 90% magnetic components in the ^{151}Eu and ^{153}Eu Mössbauer spectra are in excellent agreement ($x=0$ in

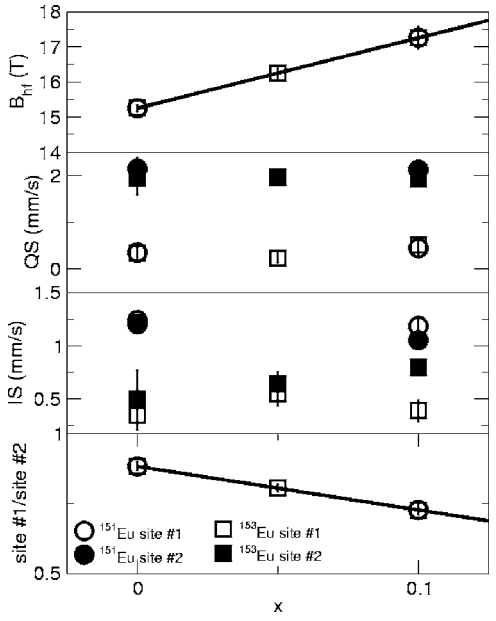

FIG. 8. Doping dependence of the fitted hyperfine parameters for the ^{151}Eu and ^{153}Eu spectra of $Eu_2BaZn_xNi_{1-x}O_5$. Solid lines are guides to the eye. Values are derived from the dynamic model described in the text.

Fig. 8), a clear indication that the base temperature analysis is fully self-consistent and that the same Eu^{3+} moments are being measured by each isotope. At high temperatures, spectra for both Eu Mössbauer isotopes show a single broad line (Fig. 7). The spectra evolve on cooling such that the hyperfine field appears to become larger and linewidths narrower, until at base temperatures (bottom spectra in Fig. 7) the full set of lines can be resolved and fitted with Γ_{nat}.

Unlike the static field distribution described above, the temperature development of the spectra on cooling is completely described by a single fitting parameter, ν, that represents the Eu^{3+} moment fluctuation rate.[4] Figure 1 shows the fitted values for $\nu(T)$. At high temperatures, the exchange induced Eu^{3+} moments (from the Ni ions in the one dimensional quantum spin chains) fluctuate rapidly and this results in a time averaged $B_{hf} \sim 0$ T so that a single broad spectral line is observed (Fig. 7). $\nu(T)$ decreases on cooling and the time averaged B_{hf} becomes larger, and this behavior is mirrored in the sharpening of the spectral lines with decreasing temperature. Finally, by ~ 5 K the Ni^{2+} are static and $\nu=0$. Independent fits of the ^{151}Eu and ^{153}Eu spectra provide exactly the same $\nu(T)$ behavior (Fig. 1). This striking agreement between $\nu(T)$ for the two isotopes is unequivocal evidence of the correctness of our description of the physics underlying the magnetism during the ordering process of this R^{3+}-Ni^{2+} Haldane quantum spin chain system.

The lifetimes of the ^{151}Eu and ^{153}Eu Mössbauer isotopes in an excited state are significantly different, as shown by their Γ_{nat} (e.g., $t_{1/2}=9.5$ ns for ^{151}Eu and $t_{1/2}=3.88$ ns for ^{153}Eu[23]). If the magnetically disordered state of quantum spin chains in a Haldane system were similar to that seen in conventional magnets (where fluctuations occur at all time and lengths scales above the critical temperature, T_C) then $\nu(T)$ would not be identical (until $T \sim T_C$) since each isotope would be most sensitive to the population of spins that are oscillating in its measuring time window (determined by $t_{1/2}$). This $\nu(T)$ agreement between the two Eu isotopes is evidence that while the Ni^{2+} ions in the spin chains exist in a quantum disordered state that should not magnetically order even at $T=0$, the fluctuations are likely coherent and occur within a small range of energies.

C. The effects of Zn doping

Characteristic ^{151}Eu and ^{153}Eu transmission Mössbauer spectra of $Eu_2BaZn_xNi_{1-x}O_5$ for $x=0$, 0.05, and 0.1 are shown in Figs. 9 and 10, respectively. Replacing Ni^{2+} with Zn^{2+} does not alter the crystal structure as determined by x-ray diffraction (not shown), and the consistency of both the isomer shift and the quadrupole splitting (Fig. 8) indicates that Zn is replacing Ni in the one dimensional quantum spin chains. The nonmagnetic Zn impurities break the Ni chains into shorter units and lead to a clear increase in the Haldane gap energy Δ with x (inset to Fig. 3) consistent with recent predictions.[22,26]

The impact of shortening the Ni^{2+} chains is clearly observable in the base temperature ^{151}Eu spectra shown in Fig. 9. Although the hyperfine field pattern is unmistakable in the $x=0$ spectrum, doping with $x=0.1$ Zn^{3+} ions washes out the

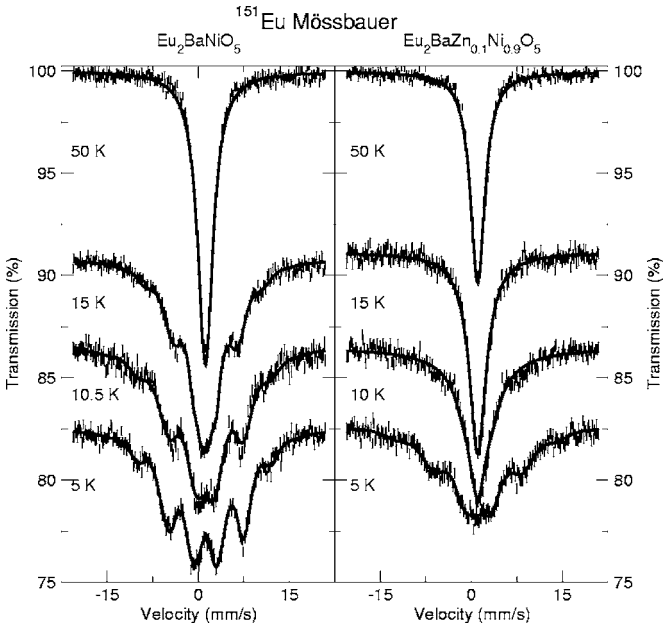

FIG. 9. Typical ^{151}Eu Mössbauer spectra for $Eu_2BaZn_xNi_{1-x}O_5$ ($x=0$ and 0.1). Solid lines are dynamic fits as described in the text.

signature of the individual nuclear transitions. While less obvious in the low temperature spectra ^{153}Eu in Fig. 10, there is a clear evolution of an asymmetric component to the lineshape with increasing x that is due to paramagnetic Eu ions in addition to a decrease in the spectral weight of the ordered component (site ratios shown in Fig. 8).

The fitted Eu^{3+} moment fluctuation rate as a function of temperature is shown in Fig. 11 on a lin-log scale for both ^{151}Eu and ^{153}Eu. Again, there is excellent agreement between the measurements made with the two Mössbauer isotopes,

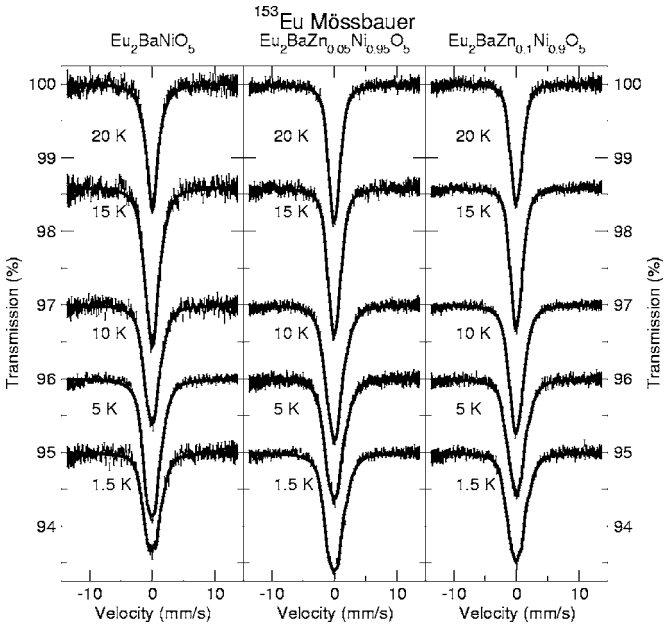

FIG. 10. Typical ^{153}Eu Mössbauer spectra for $Eu_2BaZn_xNi_{1-x}O_5$ ($x=0$, 0.05, and 0.1). Solid lines are dynamic fits as described in the text.

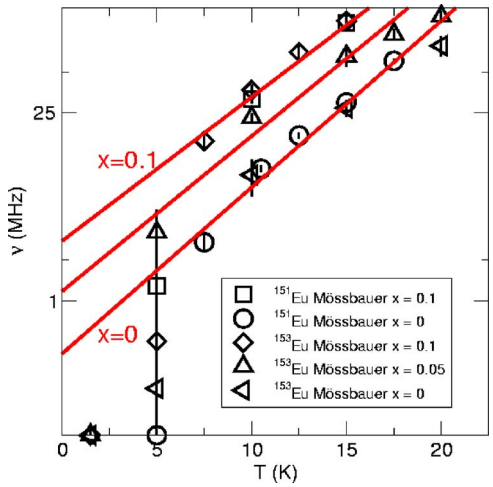

FIG. 11. (Color online) Eu^{3+} moment fluctuation rate (ν) as a function of temperature and doping concentration x determined from dynamic fits to the Mössbauer spectra. Solid lines are to fits described in the text.

confirming that the underlying physical processes are being described correctly.

To better understand these results, we consider the valence bond solid (VBS) model[27] of an antiferromagnetic $S=1$ Heisenberg system, where nonmagnetic impurities (here Zn) should produce an ensemble of finite length chain segments with a Haldane gap that increases with decreasing chain length[22] as well as localized $S=1/2$ spins at the chain ends[28] (although in real $S=1$ chains experimental evidence points to the existence of effective $S=1/2$ degrees of freedom that occur in $S=0$ and 1 pairs[29]). Effectively, chain severing implies that there is a discretization of the kinetic energy of the excitations (e.g., magnons) in the quantum spin chains. That is, a doped $S=1$ system can be considered to be a distribution of dimers with ferro- and antiferromagnetic interdimer couplings.[26]

Further insight into the quantum spin chain dynamics is provided by the $\nu(T)$ data in Fig. 11. Cutting the quantum spin chains into smaller chain segments results in the Eu^{3+} moments flipping more rapidly at any given temperature. This interpretation is from Eu^{3+} moments that are exchange induced by the Ni^{2+} moments, so that severing the chains with Zn doping results in faster dynamics within the chain segments. Similar behavior has been observed using neutron scattering on chain broken $Y_{2-x}Ca_xBaNi_{1-y}Zn_yO_5$ (Refs. 26 and 30) and muon spin relaxation in chain broken $Y_{2-x}Ca_xBaNi_{1-y}Mg_yO_5$.[21] Furthermore, recent inelastic neutron scattering work on $Y_2BaNi_{1-x}Mg_xO_5$ (Ref. 26) has shown that shorter chain lengths lead to an upward renormalization of the Haldane gap energy, where transitions between quantum states are shifted to higher energies for shorter chain lengths. A shift towards higher energies indicates that the dynamics of the system are moving to shorter times which is consistent with our observation of increasing relaxation rates caused by Zn doping (Fig. 11).

The exponential temperature dependence of $\nu(T)$, suggests that a thermally activated process is responsible for the moment fluctuations (that may be due to transitions between the quantum states that represent fluctuations between the ferro- or antiferromagnetic interdimer coupling) of the Ni^{2+} ions measured by way of the exchange induced Eu^{3+} moments. The data in Fig. 11 may be fitted (solid lines) to an Arrhenius relation $\nu(T)=\alpha\exp[-\Delta E/(k_BT)]$ where α is a scaling factor, k_B is Boltzmann's constant and T the temperature. ΔE decreases approximately linearly from ~3.5 meV at $x=0$ to ~1.7 meV at $x=0.1$.

Neutron scattering measurements on doped $Y_2BaNi_{1-x}Zn_xO_5$ (Ref. 31) also found evidence for thermally activated fluctuations of the Ni^{2+} moments, and that these fluctuations were also affected by chain length. These results are fully consistent with the behavior that we observe at the Eu^{3+} sites. In addition, our fitted values for ΔE are similar to the spin wave scattering energy (of magnon fluctuations that are due to moment oscillations in the quantum spin chains from the different interdimer couplings) in Nd_2BaNiO_5 (Ref. 1) and Pr_2BaNiO_5.[32] Decreasing the average chain length by increasing x seems to reduce the energy required for quantum spin fluctuations, and this is mirrored in the faster observed fluctuation rates that we observe at any given temperature. Recent studies of the affects of chain end defects in $Y_2BaNi_{1-x}Mg_xO_5$ indicate the presence of interchain segment interactions. If similar behavior is present with chain cutting in $Eu_2BaZn_xNi_{1-x}O_5$, it is possible that interactions between chain segments become stronger with decreasing chain length. More energetic interactions between chain segments would lower the energy required for transitions between the ferro- or antiferromagnetic interdimer coupling described above, that results in a faster fluctuation rate at a temperature.

It has been proposed that cutting the quantum spin chains may provide a mechanism for the spin chain moments to evolve from a quantum disordered state to an antiferromagnet or spin-glass.[26] Progression from a disordered state to an antiferromagnet or spin-glass with chain severing should be marked by a modification of the rate of change of Ni^{2+} moment fluctuations with temperature (i.e., $\Delta\nu/\Delta T$). However, the slopes of the $\nu(T)$ data above T_N (solid lines in Fig. 11) remain essentially unchanged with x, indicating that interchain coupling is not significantly altered by chain severing.

Finally, from the fitted B_{hf} for the different dopings, there is a trend of increasing Eu^{3+} moment size with decreasing Ni^{2+} chain length (Fig. 8) that results in ~25% increase in B_{hf} as x increases from 0.0 to 0.1. As the Eu^{3+} moment is exchange-induced by interactions with the Ni^{2+} chain moments, the larger Eu^{3+} moment indicates an increase in the average molecular field from the Ni^{2+} ions in the quantum spin chains. This larger molecular field can be interpreted in terms of the VBS model where severed chain ends tend to bias the polarization of the Ni ions towards ferromagnetic interdimer couplings that would increase the average measured field in the system. Despite the increase in the exchange-induced Eu^{3+} moment, we observe no change in T_N. However, the R moment dependence of T_N is essentially flat at small R moments (Fig. 1), so with Eu^{3+} moments of order 0.2 μ_B, even a ~25% increase is expected to have no measurable impact on T_N.

IV. CONCLUSIONS

By exploring the local rare earth magnetism using two independent probes of the Eu^{3+} (and hence Ni^{2+}) environments with ^{151}Eu and ^{153}Eu Mössbauer isotopes, and consistently matching our atomic level description of the magnetism with the bulk (e.g., dc and ac susceptibility) properties we have been able to examine the quantum spin chain development with temperature and chain length in $Eu_2BaZn_xNi_{1-x}O_5$ for $x=0, 0.05$, and 0.1. We have demonstrated that the Ni^{2+} ion quantum spin chains undergo magnetic relaxation with a fluctuation rate that decreases with temperature as T_N is approached on cooling. The Ni^{2+} moments are static below $T_N \sim 5$ K. Furthermore, T_N remains unaffected by the quantum spin chain length, behavior that is consistent with the R driven ordering due to the T^{-1} divergence of the R bare susceptibility. Lastly, a thermal activation energy dependence for the Ni^{2+} spin correlations and fluctuations was measured, with the energy required for a moment oscillation decreasing with shorter Ni^{2+} chain length. These results provide strong evidence for the absence of any possible antiferromagnetic or spin-glass transition at any temperature due to the interchain interactions. Furthermore, severed chain ends appear to bias the polarization of the Ni ions in the quantum spin chains.

ACKNOWLEDGMENTS

We are grateful to G. Kennedy and the staff of the SLOWPOKE Reactor Laboratory at École Polytechnique Montréal, for neutron irradiation of the $^{152}Sm_2O_3$ used in the preparation of the ^{153}Eu Mössbauer sources. This work was supported by grants from the Natural Sciences and Engineering Research Council of Canada, Fonds pour la formation de chercheurs et l'aide á la recherche, Québec and the Australian Research Council.

[1] A. Zheludev, S. Maslov, T. Yokoo, S. Raymond, S. E. Nagler, and J. Akimitsu, J. Phys.: Condens. Matter **13**, R525 (2001).
[2] J. V. Alvarez and R. Valenti, Eur. Phys. J. B **44**, 439 (2005).
[3] G. A. Stewart, S. J. Harker, M. Strecker, and G. Wortmann, Phys. Rev. B **61**, 6220 (2000).
[4] C. J. Voyer, J. van Lierop, D. H. Ryan, and J. M. Cadogan (unpublished).
[5] Y. A. Hadjiiskii, I. V. Paukov, M. N. Popova, and B. V. Mill, Phys. Lett. A **189**, 109 (1994).
[6] J. A. Hodges and P. Bonville, J. Phys.: Condens. Matter **16**, 8661 (2004).
[7] A. Frank, Phys. Rev. **39**, 119 (1932).
[8] J. van Lierop and D. H. Ryan, Phys. Rev. B **65**, 104402 (2002).
[9] A. Zheludev, S. Maslov, T. Yokoo, J. Akimiwtsu, S. Raymond, S. E. Nagler, and K. Hirota, Phys. Rev. B **61**, 11601 (2000).
[10] L. Cranswick, M. Potter, and D. H. Ryan (unpublished).
[11] A. C. Larson and R. B. Von Dreele, Los Alamos National Laboratory Report LAUR 86, 748 (2000).
[12] B. H. Toby, J. Appl. Crystallogr. **34**, 210 (2001).
[13] J. Darriet and L. P. Regnault, Solid State Commun. **86**, 409 (1993).
[14] T. Yokoo, T. Sakaguchi, K. Kakurai, and J. Akimitsu, J. Phys. Soc. Jpn. **64**, 3651 (1995).
[15] I. Affleck, Phys. Rev. B **41**, 6697 (1990).
[16] L.-P. Regnault, I. A. Zaliznyak, and S. V. Meshkov, J. Phys.: Condens. Matter **5**, L677 (1993).
[17] J. Rodríguez-Carvajal, Physica B **192**, 55 (1993).
[18] *Neutron Data Booklet*, 2nd ed., edited by A. J. Dianoux and G. Lander (OCP Science, Philadelphia, 2003), Chap. 2.5.
[19] E. Garcia-Matres, J. L. Martinez, and J. Rodríguez-Carvajal, Eur. Phys. J. B **24**, 59 (2001).
[20] I. Nowik and S. Ofer, Phys. Rev. **153**, 409 (1967).
[21] K. Kojima, A. Keren, L. P. Lee, G. M. Luke, B. Nachumi, W. D. Wu, Y. J. Uemura, K. Kiyono, S. Miyasaka, H. Takagi, and S. Uchida, Phys. Rev. Lett. **74**, 3471 (1995).
[22] S. R. White and D. A. Huse, Phys. Rev. B **48**, 3844 (1993).
[23] G. J. Long and F. Grandjean, *Mössbauer Spectroscopy Applied to Inorganic Chemistry* (Springer, New York, 1984).
[24] B. Window, J. Phys. E **4**, 401 (1971).
[25] M. Blume and J. A. Tjon, Phys. Rev. **165**, 446 (1968).
[26] M. Kenzelmann, G. Xu, I. A. Zaliznyak, C. Broholm, J. F. DiTusa, G. Aeppli, T. Ito, K. Oka, and H. Takagi, Phys. Rev. Lett. **90**, 087202 (2003).
[27] I. Affleck, T. Kennedy, E. H. Lieb, and H. Tasaki, Phys. Rev. Lett. **59**, 799 (1987).
[28] E. S. Sørensen and I. Affleck, Phys. Rev. B **51**, 16115 (1995).
[29] A. P. Ramirez, S. W. Cheong, and M. L. Kaplan, Phys. Rev. Lett. **72**, 3108 (1994).
[30] J. F. DiTusa, S. W. Cheong, J. H. Park, G. Aeppli, C. Broholm, and C. T. Chen, Phys. Rev. Lett. **73**, 1857 (1994).
[31] F. J. Mompeán, M. García-Hernández, J. L. Martínez, E. García-Matres, C. Prieto, A. D. Andrés, R. Sáez-Puche, R. S. Eccleston, and H. Schober, Physica B **234-236**, 572 (1997).
[32] A. Zheludev, J. M. Tranquada, T. Vogt, and D. J. Buttrey, Phys. Rev. B **54**, 6437 (1996).